Seasonal and solar activity variations of the Weddell Sea Anomaly observed in the TOPEX total electron content measurements

G. Jee,[1] A. G. Burns,[2] Y.-H. Kim,[3] and W. Wang[2]

Received 5 October 2008; revised 14 January 2009; accepted 3 February 2009; published 7 April 2009.

[1] The Weddell Sea Anomaly (WSA) in the ionosphere is characterized by higher plasma densities at night than during the day in the region near the Weddell Sea. According to previous studies on the WSA, it is known to occur mostly in southern summer and has not been reported in other seasons. We have utilized more than 13 years of TOPEX total electron content (TEC) measurements in order to study how the WSA varies with seasons and how it changes with solar activity. The TOPEX TEC data have been extensively utilized for climatological studies of the ionosphere because of their excellent spatial and temporal coverage. We investigate the seasonal and solar activity variations of the WSA using four seasonal cases (March equinox, June solstice, September equinox, and December solstice) and two solar activity conditions ($F10.7 < 120$ for solar minimum and $F10.7 > 120$ for solar maximum conditions) for geomagnetically quiet periods. Our analysis shows that (1) the WSA occurs only in the southern summer hemisphere for low $F10.7$, as in previous studies, but (2) the WSA occurs in all seasons except for winter when $F10.7$ is high; it is most prominent during the December solstice (southern summer) and still strong during both equinoxes. The TOPEX TEC maps in the midlatitude and high-latitude ionosphere display significant global longitudinal variations for a given local time in the Southern Hemisphere, which varies with season and solar activity. The observed WSA appears to be an extreme manifestation of the longitudinal variations.

Citation: Jee, G., A. G. Burns, Y.-H. Kim, and W. Wang (2009), Seasonal and solar activity variations of the Weddell Sea Anomaly observed in the TOPEX total electron content measurements, *J. Geophys. Res.*, *114*, A04307, doi:10.1029/2008JA013801.

1. Introduction

[2] Since it was discovered in the late 1950s and early 1960s [*Bellchambers and Piggott*, 1958; *Penndorf*, 1965], the Weddell Sea Anomaly (WSA) has not received much attention in the ionospheric community. In the last decade and a half, space-based observations of the global ionospheric plasma densities have become available, which has permitted some studies of the WSA over the ocean near the Antarctic Peninsula [*Horvath and Essex*, 2003; *Horvath*, 2006]. Early studies based on the ground-based observations [e.g., *Penndorf*, 1965] did not give such an overall picture of the WSA, including its spatial and temporal scales, as most of the features associated with the WSA occur over the ocean. Even GPS total electron content (TEC) measurements, one of the most widely utilized set of satellite observations for the global ionosphere, are not able to depict the WSA because they are also based on a ground receiver network, which is relatively sparse in the Southern Hemisphere as it is dominated by oceans [*Mannucci et al.*, 1998; *Hernandez-Pajares et al.*, 1999]. Therefore, the complete spatial morphology of the WSA was not discovered until *Horvath and Essex* [2003] reported it using the TEC data over the ocean from the TOPEX/Poseidon mission during 1998/1999 near sunspot maximum. The daytime and nighttime phenomena of the WSA were described separately by using the TEC data in two different seasonal conditions; daytime for vernal equinox and nighttime for summer. In their follow-up study [*Horvath*, 2006] the nighttime WSA was investigated using the same TOPEX TEC data, but for different periods of time; 1996/1997 only during summer. They reported the spatial distributions and the local time variations of the nighttime WSA with plausible speculations on the possible physical mechanisms responsible for producing the anomaly. More recently, *Burns et al.* [2008] utilized the ionospheric data from the Constellation Observing System for Meteorology, Ionosphere, and Climate (COSMIC) mission to develop global-scale climate maps of N_mF_2 and h_mF_2 during the southern summer (northern winter). Their study was focused on the relationship of the WSA to the low latitudes rather than the high latitudes and discussed the strengths and weaknesses of various possible physical mechanisms. They also discussed modeling efforts that were undertaken to simulate the WSA using the Coupled Magnetosphere Ionosphere Thermosphere (CMIT) model. These runs did not produce the WSA. Because of the weaknesses in the other mechanisms and the nighttime increases of h_mF_2 associated with the WSA, they suggested that an evening downward plasma flux from

[1] Korea Polar Research Institute, KORDI, Incheon, South Korea.
[2] High Altitude Observatory, National Center for Atmospheric Research, Boulder, Colorado, USA.
[3] Department of Astronomy and Space Science, Chungnam National University, Daejeon, South Korea.

0148-0227/09/2008JA013801$09.00

the plasmasphere may be able to explain at least partly the WSA.

[3] The WSA can be described as a state in which the nighttime plasma density is greater than the daytime density in the region near the Weddell Sea. The nighttime TEC is larger than the daytime value in a region from about 55°S to 66°S in latitude (the latter is the southern boundary of the satellite orbit), and about 225°–315° in longitude in the southern summer hemisphere, which is the mostly west of the Weddell Sea region. So far, most of studies on the WSA have been focused on the southern summer during solar minimum. Its characteristics with different seasons and solar activity levels have not discussed in detail. In this study, we will observe how the WSA appears in different seasons and how it varies with solar activity, by using the TOPEX TEC measurements for more than 13 years from August 1992 to October 2005. So far, there have been no studies that utilized a complete set of the TOPEX data to produce hourly TEC maps of the global ionosphere for various geophysical conditions. We will construct hourly global TEC maps from the TOPEX TEC data and use these maps to investigate hourly descriptions of the WSA for a given geophysical condition. In the following sections, the results of this study will be presented after brief descriptions of the TOPEX TEC data.

2. TOPEX TEC Data

[4] The TOPEX satellite measured the TEC over the oceans for more than a solar cycle, and thus has provided a good complement to conventional ionospheric measurements, such as ground-based GPS TEC observations [*Fu et al.*, 1994; *Ho et al.*, 1997; *Codrescu et al.*, 1999, 2001; *Lynn et al.*, 2004; *Jee et al.*, 2004, 2005; *Zhu et al.*, 2006; *Horvath*, 2006]. A brief introduction to the TOPEX TEC measurements will be made in this section. Details of the TOPEX/Poseidon mission can be found in previous papers including *Fu et al.* [1994] and *Jee et al.* [2004]. The TOPEX satellite was launched on 10 August 1992 and operated for about 13 years until October 2005. This satellite carried a dual-frequency radar altimeter operating at 13.6 GHz (Ku band) and 5.3 GHz (C band) simultaneously. In order to remove the ionospheric delay, the altimeter estimates the electron content along the raypath from the satellite to the sea surface by measuring the travel times of the radio waves at the two frequencies. The derived electron content is equivalent to the total electron content (TEC) of the ionosphere in a column extending from the satellite to the subsatellite reflection point on the surface of the ocean. The TOPEX satellite was orbiting the Earth at an altitude of 1336 km with an inclination angle of 66° and a period of 112 min. There are 127 orbits in each 9.916 day period (i.e., 10-day cycle: the satellite passes vertically over the same location, to within 1 km, every ten days), which was chosen as a compromise between spatial and temporal resolutions. The orbit was close to Sun-synchronous, advancing by 2° per day, and it therefore took about 90 days to cover all local times, considering both ascending and descending nodes. The original data were obtained from the NASA Physical Oceanography Distributed Active Archive center at the Jet Propulsion Laboratory (JPL PO.DAAC/NASA) and then averaged for each 18 s or about 1° of orbit along the satellite orbit. The resulting 18-s averaged data span more than 13 years including the declining phase of solar cycle 22 and the most parts of cycle 23. Therefore, this data set is suitable for the study of both the seasonal and solar activity variations in the ionosphere.

3. Development of WSA With Local Time

[5] Figure 1 shows the hourly TEC maps of the global ionosphere for each local time with 1-h bins (i.e., 0900 ∼ 1000 LT for 0900 LT map, etc.) starting from 0900 LT and continuing for the next 24 h. Two color scales are applied; their ranges are 0 ∼ 50 TECU for 0900 ∼ 1700 LT (top group) and 0 ∼ 30 TECU for 1800 ∼ 0800 LT (bottom group). These color scales are optimized for the midlatitude and high-latitude ionospheres and therefore the TECs in the equatorial region are saturated to the maximum values of each color scale. Each TEC map for a given local time represents a description of the average global ionosphere for a certain geophysical condition out of the TOPEX TEC measurements spanning more than 13 years. The 24-h TEC maps were produced in geographic coordinates for low solar activity ($F10.7 < 120$) and for geomagnetically quiet condition ($K_p < 3$) during the December solstice period (November, December, January, February). In Figure 1, each map clearly shows the spatial coverage of the TOPEX TEC data, which are distributed over the ocean between 66°S and 66°N and suitable for the observations of the ionosphere especially in the Southern Hemisphere.

[6] By using the TOPEX TEC data from 28 November 1996 to 5 February 1997 for about a 2-month period around the December solstice, *Horvath* [2006] described how the nighttime WSA develops with local time (summer in the Southern Hemisphere) when solar activity is low ($F10.7$ cm flux ∼90). They reported that the WSA begins to appear at around 1800 LT over the southeastern Pacific and southwestern Atlantic and then moves slightly westward at 2000 LT. It fully develops at around 2200 LT and remains well developed over the midnight. After local midnight, the WSA quickly fades away and becomes very small after 0200 LT. However, it should be noted that each TEC map in their study includes large temporal variations with latitude, about 12-h local time difference between the southern boundary of satellite orbit (66°S) and the northern boundary (66°N) since the data used for each TEC maps are only for a 10-day cycle of the TOPEX satellite orbit (see section 2). Therefore their TEC maps do not show snapshots of the global ionosphere for a given local time. Instead they include significant local time variations with latitude. On the other hand, although our TEC maps are not real snapshots of the global ionosphere for given local times (which is impossible from the TOPEX data), they do represent global pictures of the average ionosphere for given local time conditions. This allows us to observe the latitudinal structures of the ionosphere in both the Northern and Southern hemispheres for the same geophysical conditions.

[7] The changes of the WSA with local time in this study show basically similar variations to the work by *Horvath* [2006] but with a few differences as shown in Figure 1. In the southern midlatitude and high-latitude ionosphere the longitudinal variations are relatively small during the daytime near the December solstice, but there are significant variations during the night. In other parts of the year, the daytime variations are as large as the nighttime ones, as can be seen

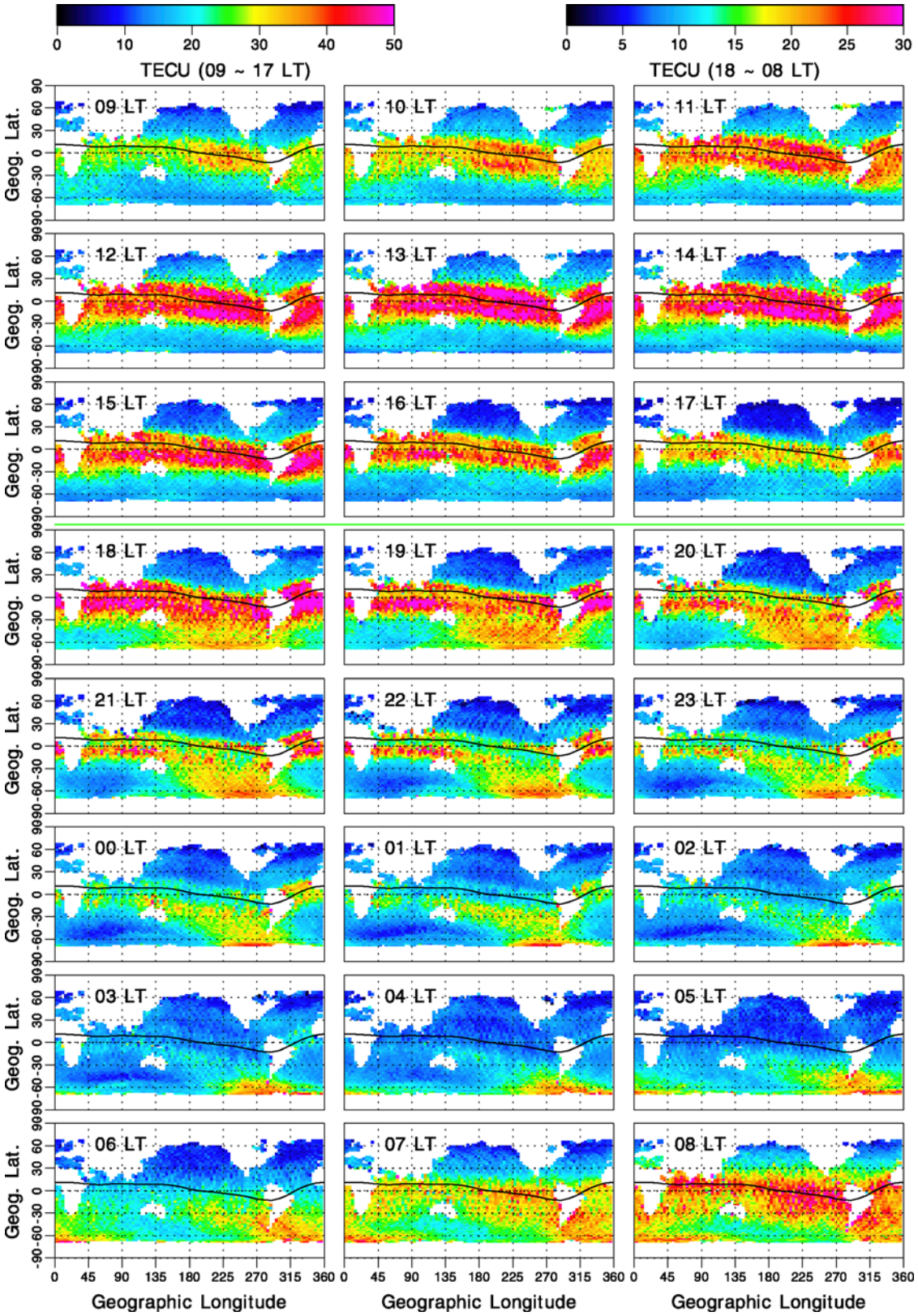

Figure 1. Local time variations of the global TEC maps with a 1-h local time bin for each map (i.e., 1200 ~ 1300 LT for 1200 MLT map, etc.) starting from 0900 LT for the next 24 h in every 1-h time interval. Each TEC map was produced in the geographic coordinate system for low solar activity ($F10.7 < 120$) and quiet conditions ($K_p < 3$) during the December solstice. Note that the color scale ranges are 0 ~ 50 TECU for 0900 ~ 1700 LT (top group) and 0 ~ 30 TECU for 1800 ~ 0800 LT (bottom group). These ranges of color scale are optimized for the midlatitude and high-latitude ionosphere.

later in this paper. The plasma densities (Figure 1) begin to decay near sunset (1800 LT), especially in the Indian and Atlantic sectors. The depletion process continues with local time and a so-called "midlatitude trough" develops over the Indian and Atlantic sectors, which becomes fully developed after midnight but disappears after about 0400 LT. However, this type of depletion process does not occur in the Pacific sector (and therefore neither does the trough); plasma densities stay high all the way through the night until dawn in this sector. Note that the nighttime TEC enhancement of the WSA does not fade away even after midnight until dawn, which is different from what *Horvath* [2006] reported, in spite of using the TEC data from the same TOPEX measurements. This difference is probably due to different periods for the TEC data. We utilized a complete set of TOPEX TEC data for more than 13 years, which is capable of showing the climatology of the ionosphere, while Horvarth's work may be showing a particular aspect of the ionosphere using the data collected only for 10-day cycle during December solstice period in 1996/1997. The longitudinal differences described here seem to result in the WSA. The density enhancements of the WSA at night initially form over the whole Pacific sector in the evening but gradually tapers to the far eastern Pacific region near the midnight and moves slightly eastward over the nighttime. The enhancement in Figure 1 appears to occur in the regions of about 50° and higher in geographic latitude and about 225° $\sim$ 315° in geographic longitude after the midnight. We also performed a similar analysis for solar maximum and found that the development of the WSA with local time is similar to its development during solar minimum as shown in Figure 1.

[8] There is an interesting aspect in the development process of the WSA, which has been pointed out by *Burns et al.* [2008]. As the WSA develops with local time (e.g., see 2100 and 2200 LT maps in Figure 1), the plasma density in the southern equatorial anomaly crest decreases in the longitude regions of the WSA, which may indicate that the plasma in the equatorial anomaly region appears to be transported to the higher latitudes, for example, via the electromagnetic force (i.e., $\mathbf{E} \times \mathbf{B}$ drift) and contribute to the density enhancement of the WSA. However, this tendency does not appear under other solar cycle or seasonal conditions (not shown); it appears only for the December solstice at solar minimum.

4. Seasonal and Solar Activity Variations

[9] In addition to the December solstice, we also analyzed the data for different seasonal conditions including the March (March, April) and September (September, October) equinoxes and the June solstice (May, June, July, August). The TEC maps for each season are shown in Figure 2 for the local noon and midnight sectors. These local time sectors were chosen to represent the daytime and nighttime ionospheres, respectively. In Figure 2, the TEC maps on the left are for solar minimum conditions, and those on the right are for solar maximum conditions. Note that the color scales are different for day and night and for solar minimum and maximum conditions to give a better representation of the features of each plot. The WSA at solar minimum appears to exist only in the December solstice (i.e., summer in the Southern Hemisphere). The WSA in summer has been observed and discussed in previous studies such as *Horvath* [2006] and *Burns et al.* [2008]. For solar maximum conditions, however, a significant density enhancement occurs in the longitudes of the WSA during both equinoxes (though it is stronger in September) as well as during the December solstice. In terms of the longitudinal variability of the ionosphere for a given local time, the low-latitude ionosphere shows relatively small variations, but the midlatitude and high-latitude ionospheres in the Southern Hemisphere show significant longitudinal variations during both day and night. It has also been reported from the study of the same 13-year TOPEX TEC measurements that the low-latitude ionosphere displays an interesting global longitudinal variability for a given local time, which is often referred to the longitudinal wave number four structure [*Scherliess et al.*, 2008; *Kim et al.*, 2008]. This longitudinal structure is supposed to appear in our TEC maps and actually can just be noticed, for instance, during June solstice in Figure 2. However, the color scales are saturated at low latitudes and more importantly, the amplitude of the wavelike structure is significantly smaller than the WSA in the global ionospheric TEC map.

[10] The longitudinal variations seem to have an opposite phase for day and night: the midlatitude and high-latitude plasma densities are smaller in the Pacific sector than in the Indian and Atlantic sectors during the day; this density variation becomes opposite during the night. Figure 3 presents the longitudinal variations of the average TECs within 50° $\sim$ 66°S GLAT for each 3.75° longitude bin, taken from the TEC maps in Figure 2. In Figure 3, the average TECs at solar minimum (top) and maximum (bottom) are plotted for each season indicated. The open symbols represent average TEC values in the local noon sector (1200 $\sim$ 1300 LT) and the filled symbols represent the midnight sector (0000 $\sim$ 0100 LT). In Figure 3, daytime and nighttime phases of the TEC variations with longitude are exactly opposite to each other for most seasons: the nighttime maximum and daytime minimum occur in roughly the same longitude region. The WSA can be understood as an extreme case of this opposite tendency between the daytime and nighttime ionospheres. Under solar maximum conditions, the nighttime longitudinal variations are significantly larger than they are at solar minimum and the WSA appears during the equinoxes in addition to the December solstice. Under solar minimum conditions, however, the nighttime longitudinal variations are relatively weak during the equinoxes and the WSA appears only in the December solstice. The December solstice period is also unique in the sense that the daytime variations are almost negligible whereas the nighttime variations are very large compared with other seasons. There are negligible nighttime variations of TEC during the June solstice, so the WSA does not appear at all during any part of the solar cycle around this solstice.

5. Discussion

[11] The original definition of an "anomaly" in the ionosphere is a departure from "solar-controlled" behavior; solar controlled behavior is defined as the condition in which the ionospheric plasma density varies regularly with the solar zenith angle [*Rishbeth*, 1998]. The anomalous density structures are very clear in Figure 3: the nighttime plasma densities are larger than the daytime densities around 270° GLON

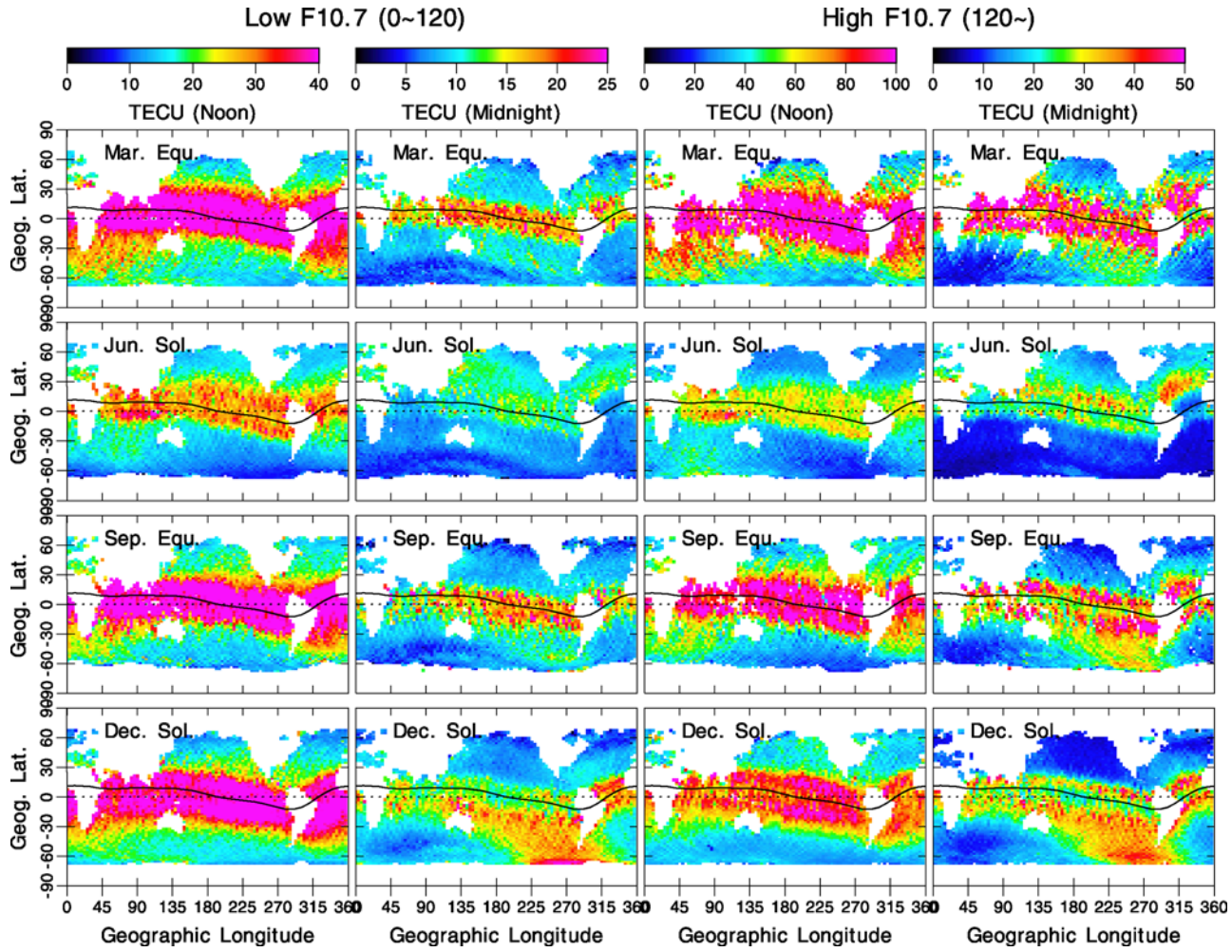

Figure 2. TEC maps for four seasonal conditions: March equinox (March, April), June solstice (May, June, July, August), September equinox (September, October), and December solstice (November, December, January, February). The TEC maps for each season are shown for the noon and midnight local time sectors as representatives of daytime and nighttime ionospheres, respectively. The TEC maps for low solar activity are on the left, and the TEC maps for high solar activity are on the right, as labeled at the top.

during the December solstice for both parts of solar cycle and during the September equinox at solar maximum, which indicates that the WSA is an anomalous diurnal variation of the midlatitude and high-latitude ionosphere in the eastern pacific region of the Southern Hemisphere. According to this definition of the WSA it seems to be inappropriate to separate it into "daytime" and "nighttime" WSAs as done by *Horvath* [2006].

[12] The development of the WSA with local time may be associated with the neutral wind effects on the plasma transport along the magnetic field line as is indicated by *Horvath* [2006]. The plasma transport by both the meridional and zonal components of the neutral winds can have a vertical component at midlatitudes and high latitudes and considerably affects the plasma densities especially at night [*Titheridge*, 1968, 1995; *Jee et al.*, 2005]. *Jee et al.* [2004] reported from their analysis of the TOPEX TEC data that there are fairly strong longitudinal variations of the TEC in the southern midlatitude (45°S MLAT) ionosphere. Although they did not make it associated with the WSA, their results were consistent with the WSA in terms of longitudinal variations for a given local time. Their interpretation of these variations was that the relatively large longitudinal changes of the magnetic declination in the southern midlatitudes are closely related with the TEC variations via the zonal wind effects which transport the plasma up and down along the magnetic field lines to regions of different recombination rates. This transport depends on the direction of both the declination and zonal wind. Figure 4 shows the magnetic declination (left) and inclination (right) obtained from the tenth generation of the International Geomagnetic Reference Field (IGRF) model. In the southern Pacific sector, the nighttime eastward zonal wind can transport the plasma upward because of the positive and large declination (red lines in Figure 4 (left)) of the magnetic field lines, whereas the effects are negligible or opposite because of small or negative declination (blue lines in Figure 4 (left)) in the other longitude sectors under the same eastward zonal wind. In addition to the zonal wind-declination effects, the meridional wind can also cause longitudinal variations of the plasma density due to the changes in inclination with longitude at middle and high latitudes (red lines in Figure 4 (right)). The longitudinal

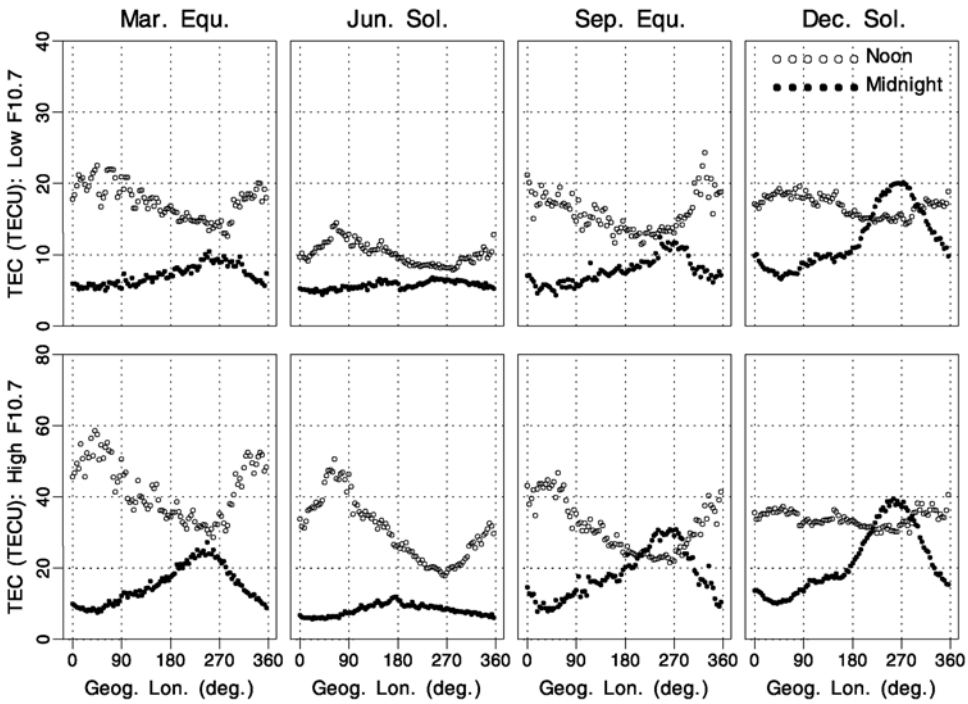

Figure 3. Longitudinal variations of the average TECs within 50° ~ 66°S GLAT for each 3.75° longitude bin, taken from the TEC maps in Figure 2. The average TECs for (top) low and (bottom) high solar activities are plotted for four seasonal cases as indicated. The open symbols represent average TEC values in the noon local time sector (1200 ~ 1300 LT) and the filled symbols in the midnight sector (0000 ~ 0100 LT).

variations of the inclination are largely related to the geographic locations of the magnetic poles. According to the IGRF, the southern magnetic pole is located at 64.5°S, 137.8°E in 2008, which results in an offset of the magnetic pole from the geographic pole of more than 15°. At high latitudes (~60° GLAT or higher), therefore, the inclination is very large, greater than 70°, in the longitude sector near the magnetic pole but relatively small, about 55°, in the longitude sectors far from the magnetic pole. The longitude of the WSA is far from the magnetic pole and the inclination is fairly small, about 55° (see Figure 4), at high latitudes so that the equatorward meridional wind can have noticeable effects on transporting the plasma upward along the field lines and contributing to the formation of the WSA. In the longitude sectors near the magnetic pole, on the other hand, the meridional wind can barely transport plasma because of very large inclination and has little effect on the plasma densities. These wind effects can be summarized by the following relation [*Titheridge*, 1995; *Rishbeth*, 1998]:

$$W_{eff} = (W_m \cos D \pm W_z \sin D) \cos I \sin I \qquad (1)$$

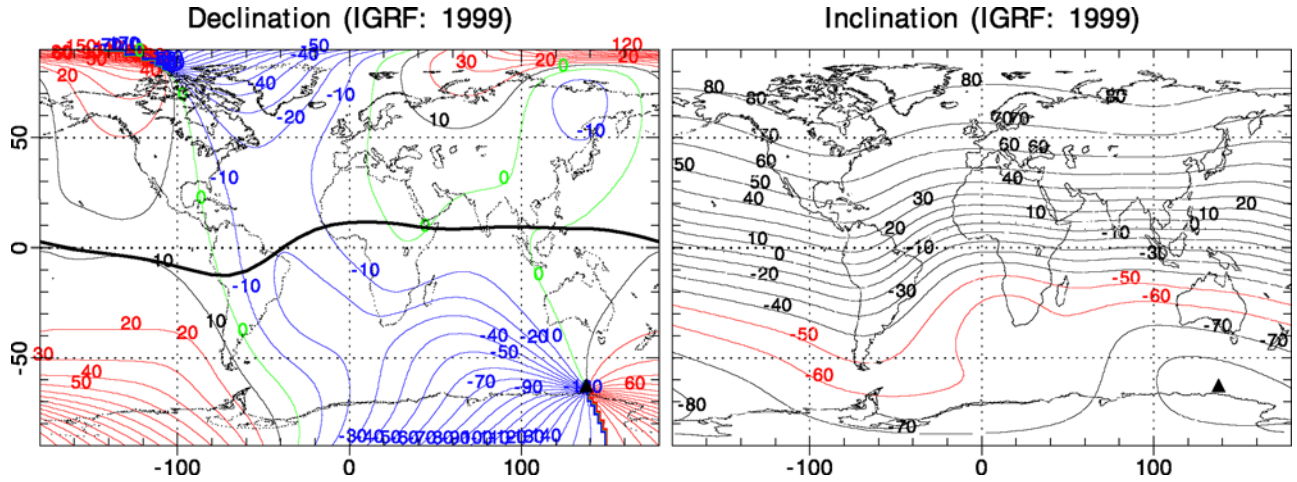

Figure 4. Geomagnetic (left) declination and (right) inclination obtained from the tenth generation of the International Geomagnetic Reference Field (IGRF) model as is in 1999.

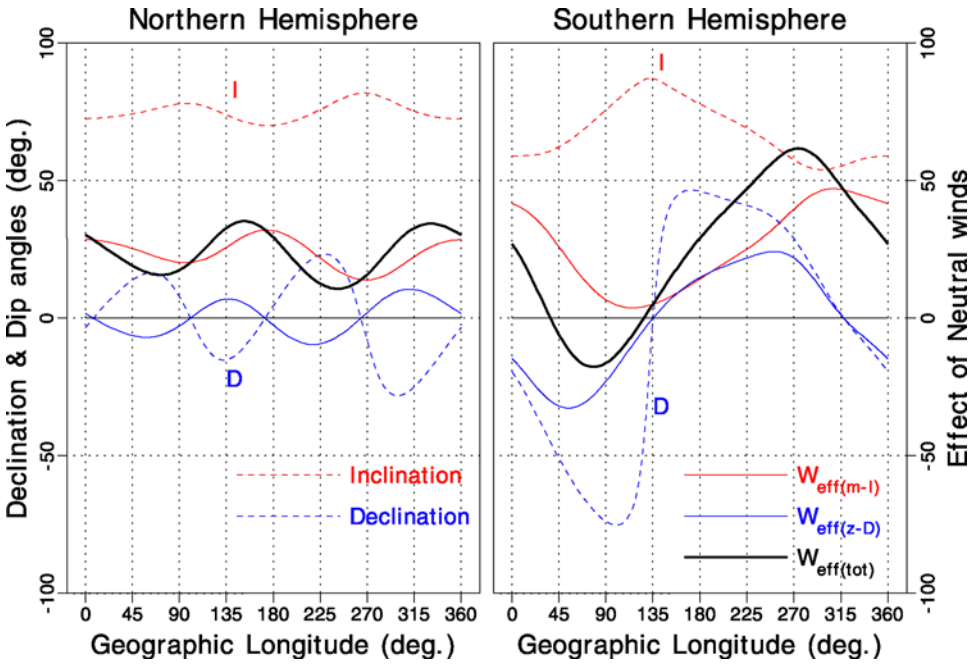

Figure 5. Estimations of the vertical components of the neutral wind effects (see equation (1)) along the geomagnetic field line at 60° GLAT in the (left) Northern and (right) Southern hemispheres: $W_{eff(m-I)}$ is the effect by the meridional wind with the inclination (thin red lines), $W_{eff(z-D)}$ is the effect by the zonal wind with the declination (thin blue lines), and $W_{eff(tot)}$ is the net effect by both winds (thick black lines). Magnetic declination (D) and inclination (I) angles are displayed with blue and red dashed lines, respectively. For this estimation, we applied the neutral winds of +100 m/s for both the equatorward and eastward winds.

where W_{eff} is the vertical component of the effective neutral wind which is capable of transporting the plasma along the magnetic field line; W_m and W_z are the meridional (+ equatorward) and zonal (+ eastward) components of neutral winds, respectively; D and I are the magnetic declination and inclination angles, respectively; + and – signs apply in the Southern and Northern hemispheres, respectively. Under the proper ion-neutral collision frequencies in the ionosphere-thermosphere system, the vertical plasma transport by the neutral winds can be estimated by W_{eff} in equation (1). Ion-neutral collision frequencies, specifically the O^+-O momentum transfer collision frequency, is an essential parameter for the coupling of the ionosphere and thermosphere and can determine the diffusion of O^+ through the neutral atmosphere in the F region and above. In order to correctly simulate the neutral wind effects on the plasma in the ionospheric model, therefore, a suitable collision frequency is required and often obtained by using the so-called "Burnside factor" to take into account the discrepancy between the theoretical calculations and the empirical values for the frequency [see *Jee et al.*, 2005; *Salah*, 1993]. Figure 5 shows the estimation of the vertical plasma transport in equation (1) with the magnetic declination (D, dashed blue lines) and inclination (I, dashed red lines) angles at 60° GLAT in the Northern (left) and Southern (right) hemispheres: $W_{eff(m-I)}$ is the effect by the meridional wind with the inclination (thin red lines), $W_{eff(z-D)}$ is the effect by the zonal wind with the declination (thin blue lines), and $W_{eff(tot)}$ is the net effect by both winds (thick black lines). We applied the neutral winds of +100 m/s for both the equatorward (W_m) and eastward (W_z) winds for this estimation. The positive values of these wind effects represent the positive effects of the neutral winds (enhancing the plasma density) and the negative values represent the negative effects (reducing the plasma density). Note that the estimations in Figure 5 are purely numerical values from equation (1) with the arbitrary, but reasonable, winds and geomagnetic parameters obtained from the IGRF. Although Figure 5 may not show any real situation, it will give us a physical insight of how the neutral winds can produce the longitudinal variations of the mid-latitude ionosphere owing to the longitudinal variations of the magnetic declination and inclination. The longitudinal variations of the neutral wind effect are relatively small in the Northern Hemisphere as expected because of relatively small longitudinal variations of the inclination and declination, but in the Southern Hemisphere they are very significant because of large longitudinal variations of the inclination and declination. The net positive effect ($W_{eff(tot)}$) peaks in the longitude of the WSA. Note that only the zonal wind can cause the negative effects on the plasma density for the applied wind, depending on the sign of the declination. When the zonal wind is relatively strong in the evening sector, the longitudinal variations of the plasma density in Figure 1 seem to be consistent with the zonal wind effect in Figure 5 in the Southern Hemisphere: the plasma densities are enhanced in the whole Pacific sector while they are reduced in the other longitude sectors. As it approaches to the midnight, the meridional wind becomes large [*Emmert et al.*, 2006; *Kawamura et al.*, 2000] and then the enhancement moves slightly eastward and narrows down to the far eastern Pacific

sector. The measurement of the h_mF_2 from COSMIC shows significant enhancements in the longitude of the WSA compared with other longitude regions [*Burns et al.*, 2008]. This enhancement of h_mF_2 is also consistent with the neutral wind effects on the ionosphere both by meridional and zonal components.

[13] The seasonal variations of the WSA found in this study seem to be physically consistent with the seasonal characteristics of the neutral winds; the nighttime equatorward wind is strongest in the summer hemisphere (i.e., the strongest WSA in summer) but the equatorward wind is weakest in the winter hemisphere (i.e., the weakest WSA in winter) [*Kawamura et al.*, 2000]. During the equinoxes, the equatorward wind at night is in between summer and winter, and so does the WSA. Furthermore, the solar ionization is still taking place even during the nighttime at high latitudes in summer [*Horvath*, 2006]. Although this ionization alone does not produce any longitudinal variation it can further enhance the WSA in summer by the meridional wind effects with the inclination (see Figure 5). In spite of the remarkable implication of the neutral wind effects on the longitudinal variations of the ionosphere including the WSA, however, it should be kept in mind that there are too few wind observations to give us evidence to support this theory.

6. Conclusion

[14] We analyzed more than 13-year TOPEX TEC data to observe the seasonal and solar activity variations of the WSA. Under solar minimum conditions, the WSA only occurs in the southern summer hemisphere as reported in previous studies. Under solar maximum conditions, however, the WSA occurs not only during the December solstice but also during the September equinox. Even during the March equinox, the nighttime TEC values are similar to the equivalent daytime values in the longitude of the WSA. The global longitudinal variation of the midlatitude and high-latitude ionospheres consists of one or two daytime peaks of TEC at longitudes distant from the WSA (one occurs fairly consistently at 45°E longitude), and a trough at the Weddell Sea longitudes. The daytime longitudinal variation is much diminished near the December solstice. It also consists of a strong nighttime peak of electron density at the longitudes of the WSA and a trough that typically occurs from 0 to 90°E. Thus the Weddell Sea anomaly is the most extreme manifestation of a global phenomenon that is seen at all longitudes, all seasons and throughout the solar cycle. The ionosphere-thermosphere community faces a significant challenge in trying to understand why the WSA is not found in current versions of the TGCMs which have proved so successful at reproducing other ionospheric and thermospheric phenomena. In addition to the neutral winds discussed in this study, there are also other factors that may contribute to producing the WSA, such as the plasmaspheric flux and electric fields. In order to better understand the WSA, extensive further research is required including observations and modeling efforts.

[15] **Acknowledgments.** This work is supported by the Integrated research on the Composition of Polar Atmosphere and Climate Change (COMPAC) under grant PE08030. A. G. Burns and W. Wang were supported by the Center for Integrated Space Weather Modeling (CISM), which is funded by the STC program under agreement ATM-0120950. NCAR is supported by the National Science Foundation. Y.-H. Kim was supported by the Korea Science and Engineering Foundation (KOSEF) grant (R01-2006-000-11003-0).

[16] Zuyin Pu thanks Ludger Scherliess and George Millward for their assistance in evaluating this paper.

References

Bellchambers, W. H., and W. R. Piggott (1958), Ionospheric measurements made at Halley Bay, *Nature*, *182*, 1596–1597, doi:10.1038/1821596a0.

Burns, A. G., Z. Zeng, W. Wang, J. Lei, S. C. Solomon, A. D. Richmond, T. L. Killeen, and Y.-H. Kuo (2008), Behavior of the F_2 peak ionosphere over the South Pacific at dusk during quiet summer conditions from COSMIC data, *J. Geophys. Res.*, *113*, A12305, doi:10.1029/2008JA013308.

Codrescu, M. V., S. E. Palo, X. Zhang, T. J. Fuller-Rowell, and C. Poppe (1999), TEC climatology derived from TOPEX/POSEIDON measurements, *J. Atmos. Sol. Terr. Phys.*, *61*, 281–298, doi:10.1016/S1364-6826(98)00132-1.

Codrescu, M. V., K. L. Beierle, T. J. Fuller-Rowell, S. E. Palo, and X. Zhang (2001), More total electron content climatology from TOPEX/Poseidon measurements, *Radio Sci.*, *36*, 325–333, doi:10.1029/1999RS002407.

Emmert, J. T., M. L. Faivre, G. Hernandez, M. J. Jarvis, J. W. Meriwether, R. J. Niciejewski, D. P. Sipler, and C. A. Tepley (2006), Climatologies of nighttime upper thermospheric winds measured by ground-based Fabry-Perot interferometers during geomagnetically quiet conditions: 1. Local time, latitudinal, seasonal, and solar cycle dependence, *J. Geophys. Res.*, *111*, A12302, doi:10.1029/2006JA011948.

Fu, L. L., E. J. Christensen, and C. A. Yamarone Jr. (1994), TOPEX/Poseidon mission overview, *J. Geophys. Res.*, *99*, 24,369–24,381, doi:10.1029/94JC01761.

Hernandez-Pajares, M., J. M. Juan, and J. Sanz (1999), New approaches in global ionospheric determination using ground GPS data, *J. Atmos. Sol. Terr. Phys.*, *61*, 1237–1247, doi:10.1016/S1364-6826(99)00054-1.

Ho, C. M., B. D. Wilson, A. J. Mannucci, U. J. Lindqwister, and D. N. Yuan (1997), A comparative study of ionospheric total electron content measurements using global ionospheric maps of GPS, TOPEX radar, and the Bent model, *Radio Sci.*, *32*, 1499–1512, doi:10.1029/97RS00580.

Horvath, I. (2006), A total electron content space weather study of the nighttime Weddell Sea Anomaly of 1996/1997 southern summer with TOPEX/Poseidon radar altimetry, *J. Geophys. Res.*, *111*, A12317, doi:10.1029/2006JA011679.

Horvath, I., and E. A. Essex (2003), The Weddell Sea Anomaly observed with the TOPEX satellite data, *J. Atmos. Sol. Terr. Phys.*, *65*, 693–706, doi:10.1016/S1364-6826(03)00083-X.

Jee, G., R. W. Schunk, and L. Scherliess (2004), Analysis of TEC data from the TOPEX/Poseidon mission, *J. Geophys. Res.*, *109*, A01301, doi:10.1029/2003JA010058.

Jee, G., R. W. Schunk, and L. Scherliess (2005), On the sensitivity of total electron content (TEC) to upper atmospheric/ionospheric parameters, *J. Atmos. Sol. Terr. Phys.*, *67*, 1040–1052, doi:10.1016/j.jastp.2005.04.001.

Kawamura, S., Y. Otsuka, S.-R. Zhang, and S. Fukao (2000), A climatology of middle and upper atmosphere radar observations of thermospheric winds, *J. Geophys. Res.*, *105*(A6), 12,777–12,788, doi:10.1029/2000JA900013.

Kim, E., G. Jee, and Y.-H. Kim (2008), Seasonal characteristics of the longitudinal wavenumber-4 structure in the equatorial ionosphere anomaly, *J. Astron. Space Sci.*, *25*(4), 1–12.

Lynn, K. J. W., M. Sjarifudin, T. J. Harris, and M. Le Huy (2004), Combined TOPEX/Poseidon TEC and ionosonde observations of negative low-latitude ionospheric storms, *Ann. Geophys.*, *22*, 2837–2847.

Mannucci, A. J., B. D. Wilson, D. N. Yuan, C. H. Ho, U. J. Lindqwister, and T. F. Runge (1998), A global mapping technique for GPS-derived ionospheric total electron content measurements, *Radio Sci.*, *33*, 565–582, doi:10.1029/97RS02707.

Penndorf, R. (1965), The average ionospheric conditions over the Antarctic, in *Geomagnetism and Aeronomy*, *Ant. Res. Ser.*, vol. 4, edited by A. H. Waynick, pp. 1–45, AGU, Washington, D. C.

Rishbeth, H. (1998), How the thermospheric circulation affects the ionospheric F2-layer, *J. Atmos. Sol. Terr. Phys.*, *60*, 1385–1402, doi:10.1016/S1364-6826(98)00062-5.

Salah, J. E. (1993), Interim standard for the atomic oxygen collision frequency, *Geophys. Res. Lett.*, *20*, 1543–1546, doi:10.1029/93GL01699.

Scherliess, L., D. C. Thompson, and R. W. Schunk (2008), Longitudinal variability of low-latitude total electron content: Tidal influences, *J. Geophys. Res.*, *113*, A01311, doi:10.1029/2007JA012480.

Titheridge, J. E. (1968), Maintenance of the night ionosphere, *J. Atmos. Terr. Phys.*, *30*, 1857–1875, doi:10.1016/0021-9169(68)90028-7.

Titheridge, J. E. (1995), Winds in the ionosphere—A review, *J. Atmos. Terr. Phys.*, *57*, 1681–1714, doi:10.1016/0021-9169(95)00091-F.

Zhu, L., R. W. Schunk, G. Jee, L. Scherliess, J. J. Sojka, and D. C. Thompson (2006), Validation study of the Ionosphere Forecast Model using the TOPEX total electron content measurements, *Radio Sci.*, *41*, RS5S11, doi:10.1029/2005RS003336.

A. G. Burns and W. Wang, High Altitude Observatory, National Center for Atmospheric Research, Boulder, CO 80307-3000, USA.

G. Jee, Korea Polar Research Institute, KORDI, Songdo Techno Park, 7-50, Songdo-dong, Yeonsu-gu, Incheon, 406-840, South Korea. (ghjee@kopri.re.kr)

Y.-H. Kim, Department of Astronomy and Space Science, Chungnam National University, 220 Gung-dong, Yuseong-gu, Daejeon, 305-754, Daejeon, South Korea.